Progress In Electromagnetics Research, PIER 90, 353–368, 2009

A BROADBAND SUSPENDED MICROSTRIP ANTENNA FOR CIRCULAR POLARIZATION

V. G. Kasabegoudar and K. J. Vinoy

Microwave Laboratory, ECE Department
Indian Institute of Science
Bangalore 560012, India

Abstract—In this paper we propose a circularly polarized (CP) microstrip antenna on a suspended substrate with a coplanar capacitive feed and a slot within the rectangular patch. The antenna has an axial ratio bandwidth ($< 3\,\mathrm{dB}$) of 7.1%. The proposed antenna exhibits a much higher impedance bandwidth of about 49% ($S_{11} < -10\,\mathrm{dB}$) and also yields return loss better than $-15\,\mathrm{dB}$ in the useful range of circular polarization. Measured characteristics of the antenna are in good agreement with the simulated results. The radiation patterns indicate good cross polarization rejection and low back lobe radiations. The design proposed here can be scaled to any frequency of interest.

1. INTRODUCTION

Although microstrip antennas in their basic form normally provide linear polarization, circular polarization (CP) operation may be obtained by certain modifications to the basic antenna geometry and/or feed. These modifications include adjusting the dimensions of the basic patch with one or more feeds, trimming the corners of a square patch, feeding the patch at adjacent sides, feeding the patch (rectangular) from its corner along the diagonal, and cutting a slot inside the patch [1]. Several such CP microstrip antennas are available in the literature. For example the antenna reported by [2] yields an axial ratio (AR) bandwidth of 6.3% with straight feed and increases up to 14.1% with an L-probe feed. This is a corner trimmed CP antenna with a U-shaped slot cut on the patch to ensure wide impedance bandwidth. There have been other works focusing on reducing the size of the antenna with a modest bandwidth for circular polarization

Corresponding author: V. G. Kasabegoudar (veereshgk2002@rediffmail.com).

operation [3]. On the other hand, antennas reported by [4] and [5] offer AR bandwidths of 14% and 23% respectively. However, these consist of stacked (multiple metal/dielectric) configurations and hence are considered difficult to fabricate reliably. On the other hand, the antenna reported by Liu and Kao [6], is a simple probe feed H-shaped microstrip antenna fed along its diagonal to excite the CP operation. But the AR bandwidth reported is only about 1.3%.

This group has recently reported a linearly polarized coplanar capacitive fed wideband microstrip antenna which provides input impedance bandwidth ($S_{11} < -10\,\text{dB}$) of about 50% [7]. Furthermore, we have suggested the use of fractal shaped boundaries for the radiating patch to get symmetric radiation patterns throughout the frequency band [8]. It may be recalled that fractal shapes have been suggested in the literature to design antennas with multi-frequency operation and/or to reduce the overall footprint [9–12]. In the present work we investigate circular polarization operation of such a patch antenna with fractal boundaries by introducing a suitably designed slot within. The antenna can be made to work either in right hand circular polarization (RHCP) or left hand circular polarization (LHCP) mode depending on the orientation of this slot. A somewhat similar approach has been followed in [13] where the feed strip is superscribed by a ring geometry. However this yielded a very small AR bandwidth of 0.7%. In another effort, fractal geometry with fractal slots has been reported with an axial ratio bandwidth of about 2% [14]. The current approach results in significantly higher AR bandwidth while retaining the simplicity of the feed configuration.

The basic design of the antenna is presented in the next section. Its design starts with the selection of center frequency as the design approach can be easily scaled to any frequency of interest [7]. Simulation studies to determine the dimensions of the fractal boundary and the slot are presented in Section 3. This is followed by sections on the experimental validation and conclusions of this study.

2. ANTENNA DESIGN

The geometry of the antenna is shown in Figure 1. This is basically a suspended coplanar capacitive fed microstrip antenna. Both antenna patch and the feed strip are etched on the same dielectric substrate, which is placed at a height above the ground plane. The antenna is excited by connecting a coaxial probe to the feed strip by a long pin SMA connector. The feed strip couples the energy to the radiating patch element capacitively.

The antenna was designed to operate with a center frequency of

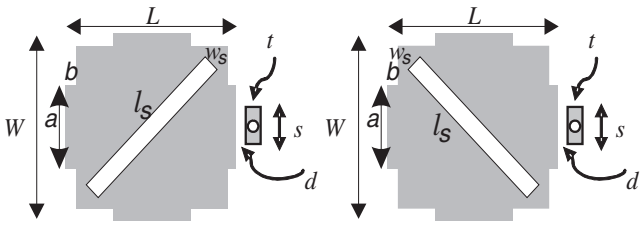

(a) Top view of RHCP and LHCP geometries

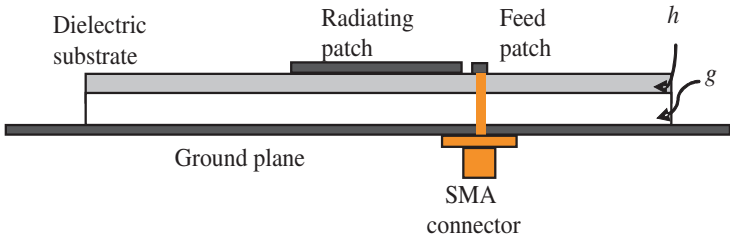

(b) Cross sectional view

Figure 1. Proposed fractal CP antenna geometry.

5.35 GHz. Radiator patch dimensions can be calculated from standard design expressions after making necessary corrections for the suspended dielectric [1, 15]. These corrections incorporate the total height above the ground $(g + h)$ and effective dielectric constant of the suspended microstrip [16]. It has been shown that the impedance bandwidth of the antenna may be maximized by using the design expression [7]

$$g \cong 0.16\lambda_0 - h\sqrt{\varepsilon_r} \tag{1}$$

where g is the height of the substrate above the ground, and h and ε_r are the thickness and dielectric constant of the substrate.

3. SIMULATION STUDIES FOR CIRCULAR POLARIZATION OPERATION

In this study we use an Arlon substrate (dielectric constant = 2.5, $\tan\delta = 0.0023$ and thickness = 1.56 mm) placed above the ground plane at a height. Initial air gap for an operational frequency of 5.35 GHz, calculated from Equation (1) is 6.25 mm. As mentioned in Section 2, the patch dimensions may be obtained using standard design expressions [1, 15]. The minimum possible width of the feed strip is 1.5 mm so that a hole can be made to connect the probe pin.

Its minimum length is approximately one fifth the side of the patch. Due to fabrication constraints the minimum separation between the patch and the feed strip is 0.2 mm. The length of the fractal projection is taken as equal to the length of the feed strip. Based on the above constraints, the physical parameters of the antenna geometry with a slot are optimized using IE3D simulations and are listed in Table 1. All these geometrical parameters (Table 1) are optimized with the IE3D which is a method of moments (MoM) based electromagnetic (EM) software by the approach explained in [7, 8]. First, optimization of dimensions of the fractal boundaries, 'a' and 'b' have been investigated to understand their effects on impedance and AR bandwidths.

Table 1. Dimensions for the antenna geometry shown in Figure 1.

Parameter	Value
Length of the radiator patch (L)	15.5 mm
Width of the radiator patch (W)	16.4 mm
Length of the feed strip (s)	5.0 mm
Width of the feed strip (t)	3.0 mm
Separation of feed strip from the patch (d)	0.5 mm
Air gap between substrates (g)	6.0 mm
Substrate thickness (h)	1.56 mm
Dielectric constant	2.5
Loss tangent	0.0023
Fractal dimension (a)	5.0 mm
Fractal dimension (b)	0.5 mm
Slot length (l_s)	15.75 mm
Slot width (w_s)	1.0 mm

The dimension 'a' is chosen equal to the length of the feed strip to have the maximum coupling and 'b' is varied from 0 to 0.9 mm, keeping all other parameters of the antenna unchanged. Return loss and AR characteristics of the antenna are depicted in Figure 2. It can be noticed from Figure 2(b) that the AR bandwidth increases with b and reaches a maximum of 7.10% for $b = 0.5$ mm. For $b > 0.5$ mm, AR bandwidth starts falling rapidly and reaches 4% for $b = 0.9$ mm. It can also be observed from Figure 2(b) that there is a shift in the center frequency of the AR band with the change in b, mainly due to change in the effective length of the patch with fractal boundaries. However the impedance bandwidth remains almost unchanged (Figure 2(a)) and is consistent with the results reported in [8]. From these studies, optimum values of 'a' and 'b' are found to be 5.0 mm and 0.5 mm, respectively.

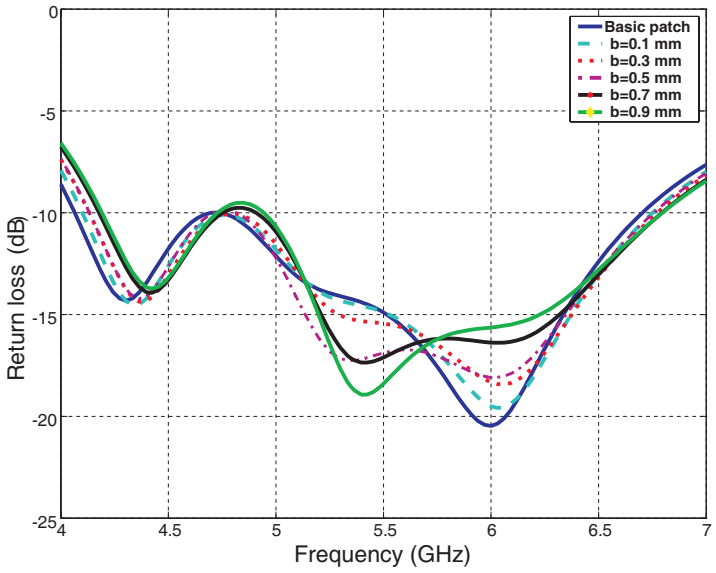

(a) Return loss characteristics

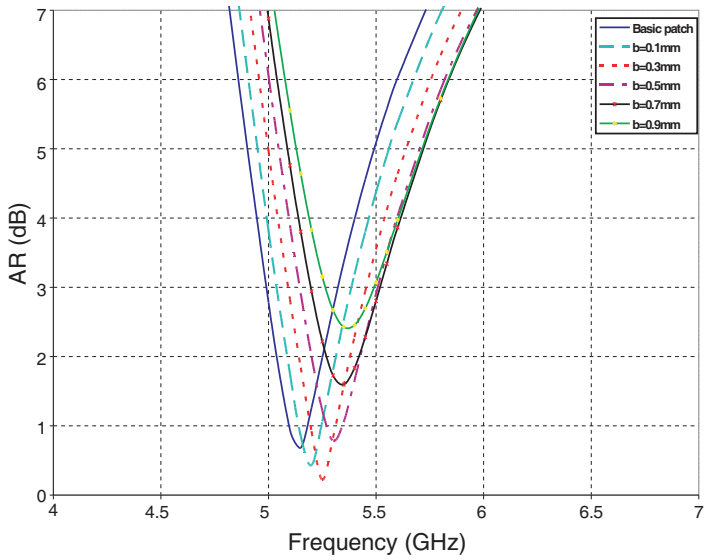

(b) AR vs. frequency characteristics

Figure 2. Performance of the circularly polarized antenna for different values of b with $a = 5.0\,\text{mm}$ constant.

Parametric studies were conducted on g, d, t and s to optimize the antenna's impedance bandwidth for fine-adjusting to obtain best possible impedance and AR bandwidth. The initial height of suspension (air gap) was calculated using (1) and then optimized. Impedance plots for different air gap values are shown in Figure 3 for the frequency range of 4 to 7 GHz. From Table 2, it can be noted that the maximum value of AR bandwidth is 7.1%. Although the impedance bandwidth obtained for $g = 5.5$ mm (49.77%) slightly higher than that for $g = 6.0$ mm (48.52%), the latter is selected as it ensures better AR bandwidth.

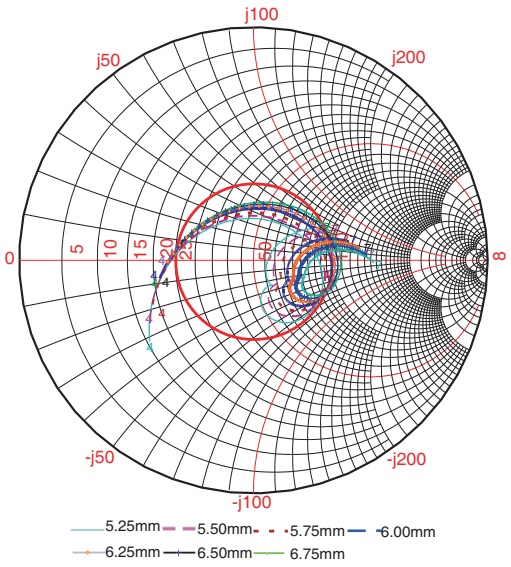

Figure 3. Impedance plot for different air gap values.

Table 2. Effect of various key design parameters on %AR BW (< 3 dB) (all geometry parameters are in mm and AR bandwidth in %). Other parameters are as listed in Table 1.

g, BW(%)	5.25, 4.13	5.50, 5.38	5.75, 6.26	6.00, 7.10	6.25, 7.05	6.50, 7.03	6.75, 7.01
d, BW(%)	0.1, 6.82	0.3, 6.84	0.5, 7.10	0.7, 6.83	1.0, 6.82	1.5, 6.79	2.0, 6.76
t, BW(%)	1.5, 6.87	2.0, 6.88	2.5, 6.89	3.0, 7.10	3.5, 6.80	4.0, 6.84	4.5, 6.80
s, BW(%)	3.0, 6.83	4.0, 6.81	5.0, 7.10	6.0, 6.89	7.0, 6.91	8.0, 6.97	9.0, 6.97

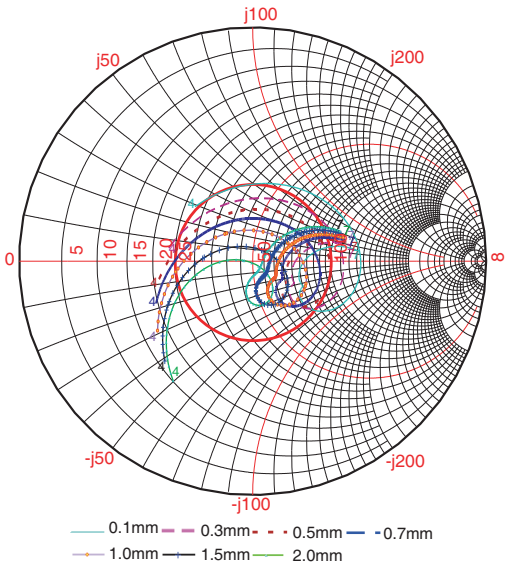

Figure 4. Impedance plot for different distances between feed strip and radiator patch.

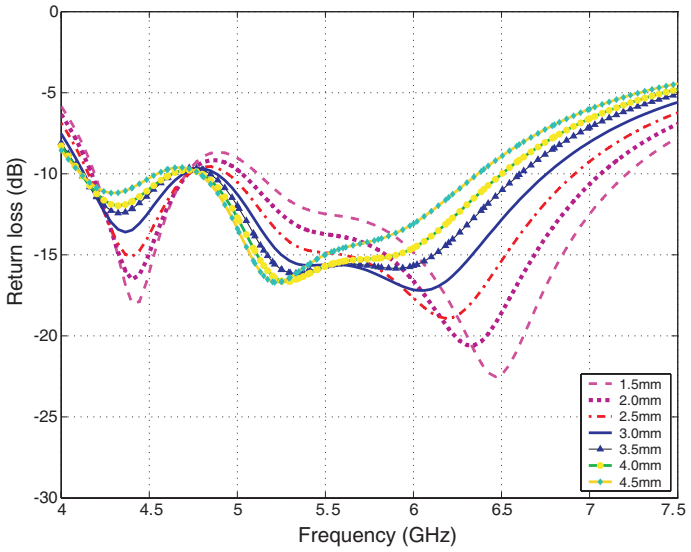

Figure 5. Effect of variation in feed strip length (t) on impedance bandwidth.

The separation between radiator patch and the feed strip (d) was varied from 0.1 mm to 2.0 mm. Effect of d on input impedance of the antenna is shown in Figure 4. It can be noted from Table 2 is that the AR bandwidth increases with d and reaches a maximum of 7.10% for $b = 0.5$ mm. Both impedance and AR bandwidth values start decreasing for $d > 0.5$ mm. From Table 2, it can be noted that, $d = 0.5$ mm is the optimum case for the AR bandwidth.

The length of the feed strip (t) was varied from 1.5 mm to 4.5 mm and the width (s) from 3.0 mm to 9.0 mm with an objective to maximize both AR and impedance bandwidth. Effect of these parameters on return loss characteristics of the antenna is shown in Figures 5 and 6 and the corresponding AR bandwidth obtained by simulations are listed in Table 2. Optimum values of the length (t) and width (s) of the feed strip are 3.0 mm and 5.0 mm, respectively.

Slot dimensions (l_s, and w_s) were also varied for the patch with the selected configuration to get the maximum axial ratio bandwidth. In the first step, slot length was optimized by keeping a slot width of 1 mm (Table 3) and later the slot width was varied to get the optimum slot dimensions (Table 4). Based on these studies it can be noted that the optimum slot length and width are 15.75 mm and 1.0 mm respectively. Simulated return loss characteristics of both LHCP and RHCP geometries are shown in Figure 7(a). For this case, the simulated 3 dB axial ratio band is from 5.16 GHz to 5.54 GHz (CP

Table 3. Effect of slot length (l_s) on AR bandwidth for slot width ($w_s = 1$ mm).

Slot length (mm)	Frequency range (AR< 3 dB) (GHz)	AR BW(%)
15.25	5.26–5.55	5.36
15.50	5.18–5.55	6.89
15.75	5.16–5.54	7.10
16.00	5.13–5.47	6.41

Table 4. Effect of slot width (w_s) on AR bandwidth for slot length ($l_s = 15.75$ mm).

Slot width (mm)	Frequency range (AR< 3 dB) (GHz)	AR BW(%)
0.90	5.16–5.53	6.92
1.00	5.16–5.54	7.10
1.10	5.15–5.52	6.93
1.25	5.13–5.50	6.96

operating range) which is about 7.1% as inferred from Figure 7(b). Minimum axial ratio of 0.52 dB was obtained at 5.35 GHz. The orientation of the slot with respect to the feed determines whether

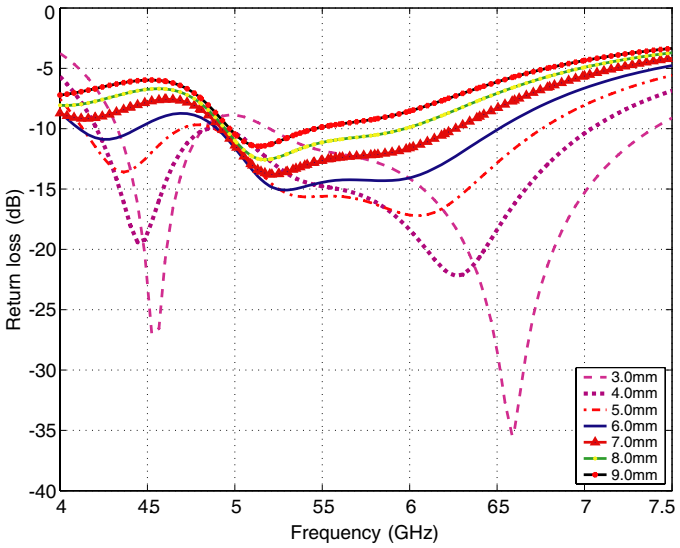

Figure 6. Effect of variation in feed strip width (s) on impedance bandwidth.

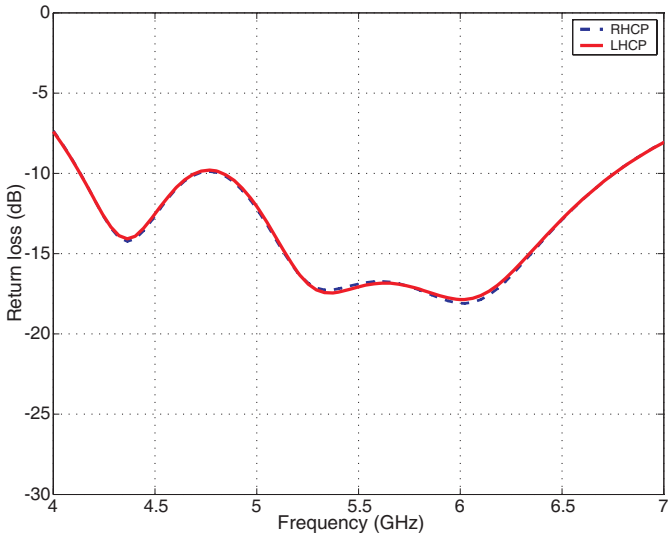

(a) Return loss characteristics

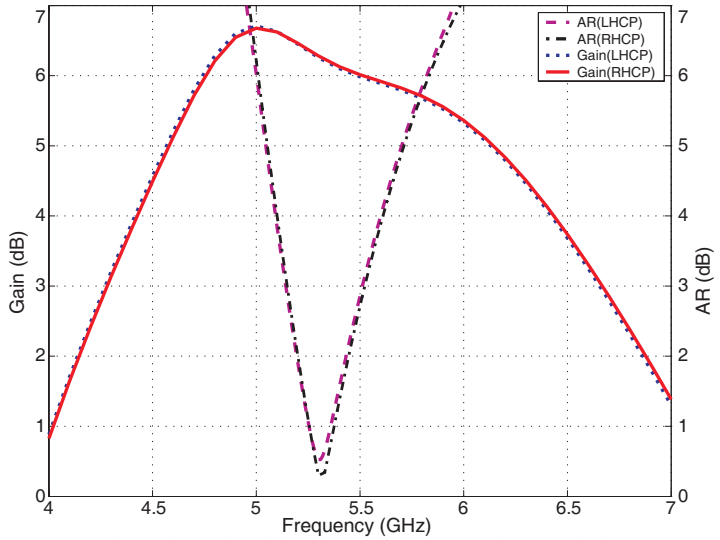

(b) Gain and axial ratio vs. frequency characteristics

Figure 7. Performance of the optimized LHCP and RHCP antennas shown in Figure 1.

the antenna operates for the left handed or right handed operation. However both options have the same geometrical parameters. From Figure 7, it can be noted that the slot orientation does not change any of the other antenna characteristics. From above studies we conclude that all characteristics of the antenna are consistent with our earlier work reported in [7, 8]. The AR bandwidth is sensitive to the change in slot dimensions (Tables 3 and 4) and while dimensions of the fractal boundary of the radiator patch (a and b) help in improving the AR bandwidth to a some extent.

Finally, the simulation study was extended to design antennas with different center frequencies to demonstrate that the proposed design is versatile and can be scaled to any frequency of interest. Two design frequencies, one on the higher side (8 GHz) and the other on the lower side (3.5 GHz) were chosen for the purpose. Summary of the designed geometry parameters, impedance bandwidth and AR bandwidth are listed in Table 5. The corresponding axial ratio characteristics are plotted in Figure 8 after normalizing with respect to these center frequencies. Almost similar performance was obtained for these two designs (Figure 8, Table 5). From the designs studied, it can be noted that circular polarization operation for this antenna can be ensured for any desired frequency as with the case reported earlier for linearly polarized antennas [7, 8].

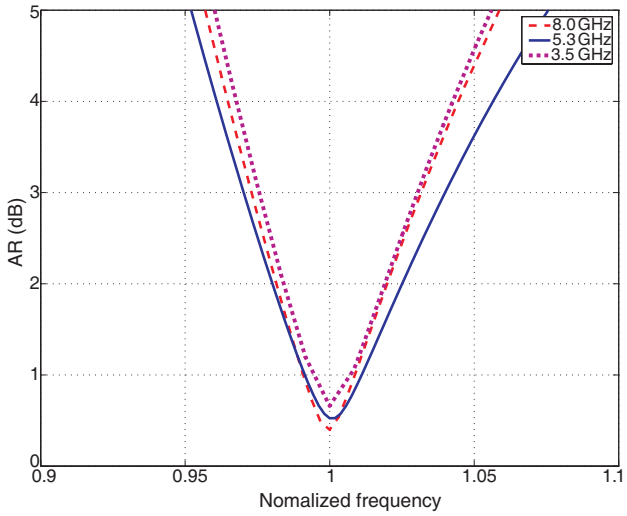

Figure 8. Simulated AR plots for different center frequencies.

Table 5. Scaling of CP antenna for different center frequencies.

Center frequency (GHz)	Geometry parameters (mm)								AR BW (%)	Impedance BW (%)
	L	W	d	s	t	g	l_s	w_s		
3.5	21.0	26.5	0.5	5.0	1.2	19.5	19.5	1.2	6.16	47.74
5.3	15.5	16.4	0.5	5.0	3.0	6.0	15.75	1.0	7.10	49.00
8.0	7.2	10.6	0.5	3.7	1.2	2.75	8.0	1.2	6.21	54.14

4. EXPERIMENTAL RESULTS

Both LHCP and RHCP prototypes were fabricated as designed in the previous section with dimensions described in Table 1 and one such prototype is shown in Figure 9. The measured return loss characteristics of the fabricated antenna in Figure 10 indicated that the return loss is below -15 dB in the CP operating range (5.16 GHz–5.54 GHz). It can be seen from these characteristics (Figure 10) that, changing the slot orientation does not affect the antenna input impedance. The radiation patterns were measured in an anechoic chamber and are plotted in Figure 11 for both LHCP and RHCP antennas at the center frequency (minimum axial ratio frequency

point). Two identical antennas each for LHCP and RHCP were fabricated to measure co and cross (opposite) polarizations. Cross polarization here indicate that the patterns measured from oppositely polarized antenna (e.g., LHCP transmitter and a RHCP receiver). Measured cross polarization levels are below −15 dB at the boresight angles and the back lobe radiations have been found to be below −20 dB for both LHCP and RHCP cases. From Figure 12, it can be noted that the measured gain of both antennas are above 4 dB in the CP range of operation. Boresight axial ratio was computed from the

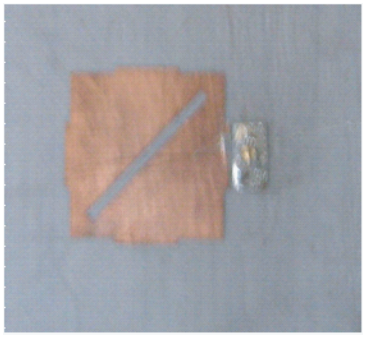

Figure 9. Fabricated prototype of geometry shown in Figure 1.

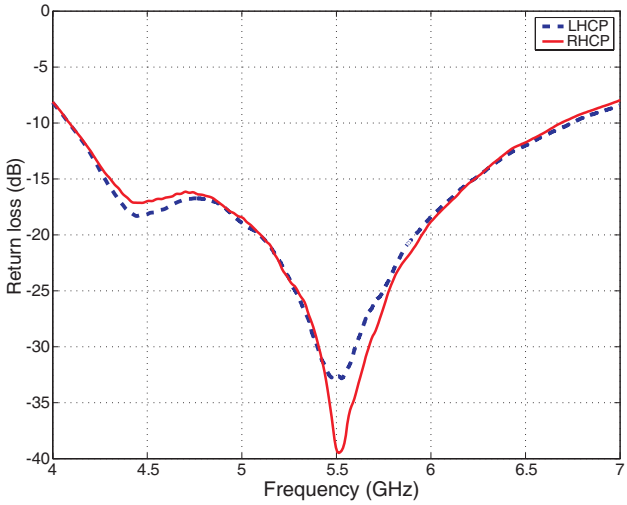

Figure 10. Measured return loss characteristics of the fabricated prototypes.

S_{21} data of LHCP and RHCP prototypes using (2) [17]. Comparisons of all results (simulated and measured) are listed in Table 6. It can be noted that measured results agree with the simulated ones.

$$AR = 20\log_{10}\left[\frac{|E_R| + |E_L|}{|E_R| - |E_L|}\right] \tag{2}$$

Table 6. Comparisons of various characteristics of simulated and fabricated prototypes.

Parameter	Simulated	Measured
Impedance bandwidth	48.52% (LHCP and RHCP)	47.58% (LHCP and RHCP)
Center frequency of the design	5.35 GHz	5.35 GHz
Return loss level in the AR band	Below −15 dB	Below −15 dB
Axial ratio bandwidth of the CP antenna	5.16–5.54 GHz (7.10%) (LHCP and RHCP)	5.20–5.59 GHz (7.22%) (RHCP) 5.19–5.58 GHz (7.24%) (LHCP)
Minimum gain in AR band	6.06 dB (LHCP and RHCP)	5.17 dB (LHCP), 4.36 dB (RHCP)
Maximum gain in AR band	6.49 dB (LHCP and RHCP)	5.67 dB (LHCP), 5.70 dB (RHCP)

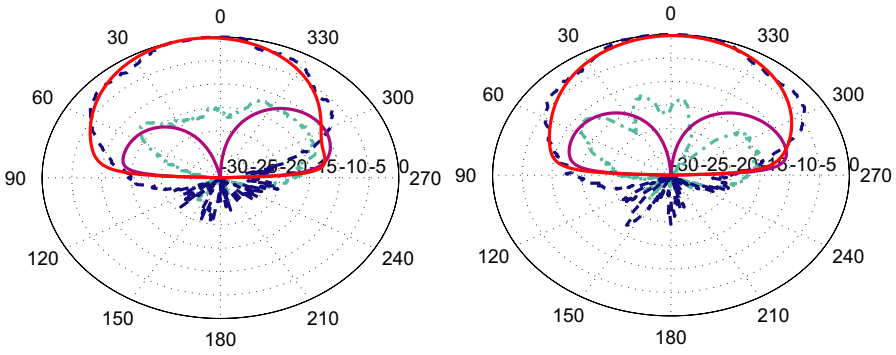

(a) Patterns of LHCP antenna in two orthogonal planes

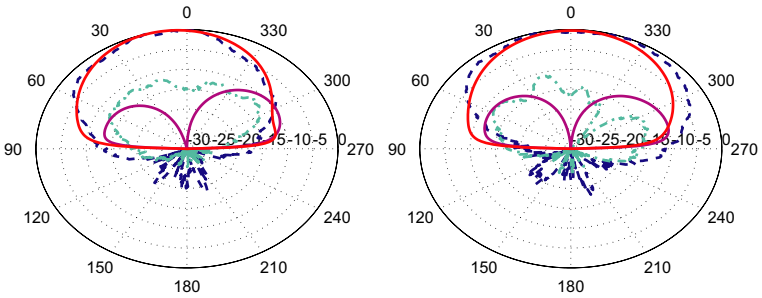

(b) Patterns of RHCP antenna in two orthogonal planes

Figure 11. Radiation patterns comparisons at 5.35 GHz. Solid curves: simulated co and cross polarizations, Dashed curves: measured co and cross polarizations.

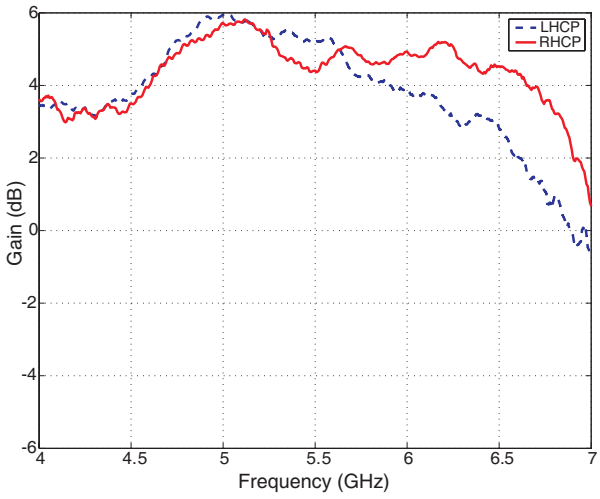

Figure 12. Measured gain vs. frequency plots of the fabricated prototypes.

5. CONCLUSIONS

The coplanar capacitive fed fractal microstrip antenna was presented for circular polarization. This feed configuration has been shown previously to improve the antenna's impedance bandwidth. The fractal geometry was used to get nearly symmetrical radiation patterns. A diagonal slot was used to excite circular polarization and slot dimensions were optimized to maximize the AR bandwidth. The

proposed geometry exhibits the return loss less than −15 dB and a gain above 4 dB in the CP operating range. Measured radiation patterns have low cross polarization and the back lobe radiation is less than −20 dB. By changing the slot orientation, antenna can be made to work in either LHCP or RHCP mode without changing any of the other parameters of the antenna. With optimum slot dimensions this antenna offers an axial ratio bandwidth of 7.1% (AR< 3 dB). It has also been established that the proposed approach can be employed to design antennas with similar performance for the desired operational frequency.

REFERENCES

1. Balanis, C. A., *Antenna Theory*, John Wiley & Sons, Inc., New York, 2004.
2. Yang, S. L. S., K. F. Lee, and A. A. Kishk, "Design and study of wideband single feed circularly polarized microstrip antennas," *PIERS Online*, Vol. 80, 45–61, 2008.
3. Chen, W. S., C. K. Wu, and K. L. Wang, "Novel compact circularly polarized square microstrip antenna," *IEEE Trans. Antennas Propagat.*, Vol. 49, No. 3, 340–342, 2001.
4. Esselle, N. K. and A. K. Verma, "Optimization of stacked microstrip antenna for circular polarization," *IEEE Antennas Wireless Propagat. Lett.*, Vol. 6, 21–24, 2007.
5. Lien, H. C., Y. C. Lee, and H. C. Tsai, "Couple-fed circular polarization bow tie microstrip antenna," *PIERS Online*, Vol. 3, No. 2, 220–224, 2007.
6. Liu, W. C. and P. C. Kao, "Design of a probe fed H-shaped microstrip antenna for circular polarization," *Journal of Electromagnetic Waves and Applications*, Vol. 21, No. 6, 857–864, 2007.
7. Kasabegoudar, V. G., D. S. Upadhyay, and K. J. Vinoy, "Design studies of ultra wideband microstrip antennas with a small capacitive feed," *Int. J. Antennas Propagat.*, Vol. 2007, No. Q4, 1–8, 2007.
8. Kasabegoudar, V. G. and K. J. Vinoy, "A wideband microstrip antenna with symmetric radiation patterns," *Microw. Opt. Technol. Lett.*, Vol. 50, No. 8, 1991–1995, 2008.
9. Vinoy, K. J., K. A. Jose, and V. K. Varadan, "On the relationship between fractal dimension and performance of multi-resonant dipole antennas using Koch curves," *IEEE Trans. Antennas Propagat.*, Vol. 51, No. 9, 2296–2303, 2003.

10. Azari, A. and J. Rowhani, "Ultra wideband fractal microstrip antenna design," *Progress In Electromagnetics Research B*, Vol. 2, 7–12, 2008.
11. Kordzadeh, A. and F. H. Kashani, "A new reduced size microstrip patch antenna with fractal shaped defects," *Progress In Electromagnetics Research B*, Vol. 11, 29–37, 2009.
12. Vinoy, K. J., K. A. Jose, V. K. Varadan, and V. V. Varadan, "Hilbert curve fractal antenna: A small resonant antenna for VHF/UHF applications," *Microw. Opt. Technol. Lett.*, Vol. 29, No. 4, 215–219, 2001.
13. Su, W., J. S. Row, and J. F. Wu, "Design of a single feed dual frequency microstrip antenna," *Microw. Opt. Technol. Lett.*, Vol. 47, No. 2, 114–116, 2005.
14. Rao, P. N. and N. V. S. N. Sarma, "A single feed circularly polarized fractal shaped microstrip antenna with fractal slot," *progress In Electromagnetics Research Symposium Proceedings*, 95–197, Hangzhou, China, Mar. 24–28, 2008.
15. Kumar, G. and K. P. Ray, *Broadband Microstrip Antennas*, Artech House, Boston, 2003.
16. Schellenberg, J. M., "CAD models for suspended and inverted microstrip," *IEEE Trans. Microw. Theo. Tech.*, Vol. 43, No. 6, 1247–1252, 1995.
17. Eldesouki, E. M. A., K. F. A. Hussein, and A. A. El-Nadi, "Circularly polarized arrays of cavity backed slot antennas for X-band satellite communications," *Progress In Electromagnetics Research B*, Vol. 9, 179–198, 2008.